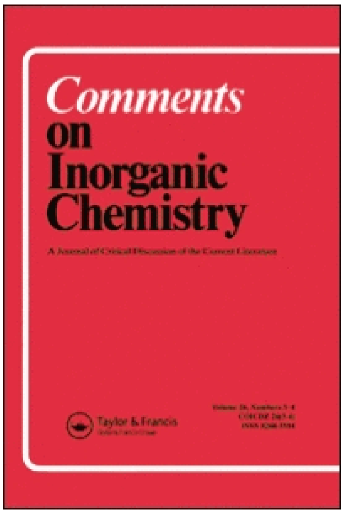

Comments on Inorganic Chemistry
Publication details, including instructions for authors and subscription information:
http://www.informaworld.com/smpp/title~content=t713455155

LUMINESCENT METALLACARBORANES

Paul A. Jelliss[a]
[a] Department of Chemistry, Saint Louis University, St. Louis, Missouri, USA

To cite this Article Jelliss, Paul A.(2008) 'LUMINESCENT METALLACARBORANES', Comments on Inorganic Chemistry, 29: 1, 1 — 25

To link to this Article: DOI: 10.1080/02603590801985208

URL: http://dx.doi.org/10.1080/02603590801985208

Comments on Inorganic Chemistry, 29: 1–25, 2008

ISSN: 0260-3594 print
DOI: 10.1080/02603590801985208

Taylor & Francis
Taylor & Francis Group

LUMINESCENT METALLACARBORANES

PAUL A. JELLISS

Department of Chemistry, Saint Louis University,
St. Louis, Missouri, USA

Metallacarborane complexes comprising MC_xB_y ($x = 1$–$3, y = 3$–10) polyhedral frameworks are not well known for their photophysical properties. While the subject of metallacarborane luminescence remains a hitherto under-explored topic, we have recently discovered surprising optoelectronic responses from a small clutch of rhenium-and ruthenium-carborane species. Thus the complexes [3,3,3-$(CO)_3$-8-I-*closo*-3,1,2-$ReC_2B_9H_{10}$]$^-$ and [3-CO-3,3-κ^2-Me_2N-$(CH_2)_2NMe_2$-*closo*-3,1,2-$RuC_2B_9H_{11}$] display low temperature (77 K) phosphorescences with single-exponential decays ($\lambda_{em} =$ 455 nm ($\tau = 1.65$ ms) and $\lambda_{em} = 450$ nm ($\tau = 0.77$ ms), respectively), while the structurally novel complex [7,10-μ-H-7-CO-7,7-$(PPh_3)_2$-*isonido*-7,8,9-$ReC_2B_7H_9$] is photoemissive in solution at ambient temperatures ($\lambda_{em} = 442$ nm) with a variable biexponential dual fluorescent decay in frozen (77 K) glass. We have also observed frozen glass and solid state blue emission ($\lambda_{em} \approx 400$ nm) from the complex [3,3-$(CO)_2$-3-NO-*closo*-3,1,2-$ReC_2B_9H_{11}$]. This work provides an opportunity to collate these results together and examine the related underlying causes for these emissions by interpretation of photophysical, electrochemical and spectroelectrochemical measurements. The results are related to the only other observed luminescence for a metallacarborane with an inclusive metal vertex, reported for the complex [*commo*-3,3′-Ni(1,2-$C_2B_9H_{11}$)$_2$], by virtue of a dynamic element leading to polyhedral skeletal reorganization of the metallacarborane framework in the excited state.

Address correspondence to Paul A. Jelliss, Department of Chemistry, Saint Louis University, 3501 Laclede Ave., St. Louis, MO 63103-2010, USA. E-mail: jellissp@slu.edu

Dedicated to the memory of Judith M. Stone (1928–2008), beloved wife of Prof. F. Gordon A. Stone.

1. INTRODUCTION

Metallacarborane complexes, where at least one of the vertices that constitute the polyhedral cage architecture is a transition metal atom, are well established in the literature thanks to the seminal work of M. F. Hawthorne and, since then, a small but charismatic group of notable proponents around the world.[1–7] Despite 40 years of reports of this class of inorganic compound, there has been little described about their photophysical properties, with a distinct paucity of information regarding luminescence. Carboranes (sans metal vertex) have nevertheless been incorporated into photophysically active metal complexes, usually as ancillary components.[8–13]

o-Carborane (*closo*-1,2-$C_2B_{10}H_{12}$) itself has been studied by Kunkely and Vogler.[14] Although non-emissive in solution at ambient temperature, solid samples displayed weak luminescence ($\lambda_{em} = 395\,nm$). On the other hand, an EtOH glass sample at 77 K was shown to be strongly blue phosphorescent ($\lambda_{em} = 441\,nm$, $\lambda_{ex} = 260\,nm$) with considerable (unassigned) vibrational structure and a very long decay lifetime ($\tau = 4\,s$). In effort to assuage criticism that this strong phosphorescence was due to an organic aromatic impurity, Kunkely and Vogler demonstrated similar vibrationally structured photoluminescent behavior ($\lambda_{em} = 462\,nm$) with the hexabromo anion [7,8,9,10,11,12-Br_6-*closo*-1-$CB_{11}H_6]^-$, albeit with a considerably shorter lifetime, $\tau < 10^{-3}\,s$.[15] This decrease in decay lifetime, along with the observation of electronic transitions at lower energy, was attributed to the presence of the bromine atoms and their associated spin-orbit coupling effect.

Laguna *et al.* have described blue photoluminescence from the *nido*-carborane diphosphines [7,8-$(PR_2)_2$-*nido*-7,8-$C_2B_9H_{10}]^-$ (R = Pr^i, Ph) as a carborane-based event that interestingly does not occur with the parent *closo* species.[16] These *nido*-carborane diphosphine ligands have also demonstrated metal-perturbed intraligand emissions when bound within trigonal-planar Au[16] and square-planar Pd[17] complexes. Their green emissions were bathochromically shifted relative to the free ligands, but were otherwise similar in appearance. The gold complexes with the [7,8-$(PPh_2)_2$-*nido*-7,8-$C_2B_9H_{10}]^-$ ligands displayed additional lower energy orange emissions attributed to metal-to-ligand charge transfer (MLCT) transitions in the gold-phosphine regime rather than the carborane.

But what of *closo*-MC_xB_y ($x = 1$–3, $y = 3$–10) metallacarboranes, where a transition metal atom is an integral vertex in the polyhedral skeletal framework, and their optoelectronic behavior? In this arena, there are few contributors and only one notable example prior to our work, which is the primary subject of this article. Perhaps quite fittingly, one of the original Hawthorne discoveries was the subject of this first report—the Ni^{IV} sandwich complex [*commo*-3,3′-$Ni(1,2\text{-}C_2B_9H_{11})_2$].[18] It was found that a corkscrew rotary motion of the carborane cage ligands relative to one another could be induced either electro- or photochemically. Of the former process, a simple one-electron reduction to Ni^{III} was sufficient to afford such rotation of the cage carbon substituents from a *cisoid* disposition to a *transoid* one. The same result was achieved by photoexcitation of the complex at $\lambda_{ex} \approx 450$ nm. Radiative relaxation occurred from the *transoid* rotor configuration, which DFT calculations showed to be more stable in the excited state, producing a very weak emission band at $\lambda_{em} \approx 900$ nm (and of course returning to the *cisoid* configuration in the ground state). The optoelectronic results from this prototypical metallacarborane complex could have important consequences for the development of molecular motor control and so-called 'nanomachines.' Indeed, as the reader will see, photoexcitation of a metallacarborane accompanied by some polyhedral skeletal rearrangement is a recurrent theme in our own work.

2. RESULTS AND DISCUSSION

2.1. Early Rhenacarborane Work

Much of our work has utilized a single precursor compound: Cs[3,3,3-$(CO)_3$-*closo*-3,1,2-$ReC_2B_9H_{11}$] (**1**) first reported by Hawthorne et al.[1] and the subject of a number of studies by Stone et al., which scrutinized the ability of the rhenacarborane complex anion to bind with a number of cationic *d*-block metal-ligand fragments.[19–21] Among the metal-metal bond-forming reactions studied was a facile and quantitative reaction with a source of the nitrosonium cation, $[NO][BF_4]$, affording the complex [3,3-$(CO)_2$-3-NO-*closo*-3,1,2-$ReC_2B_9H_{11}$] (**2**).[22]

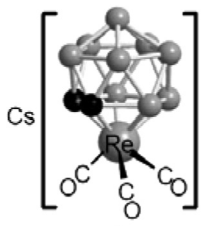

1

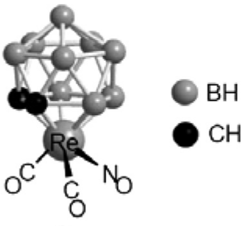

2

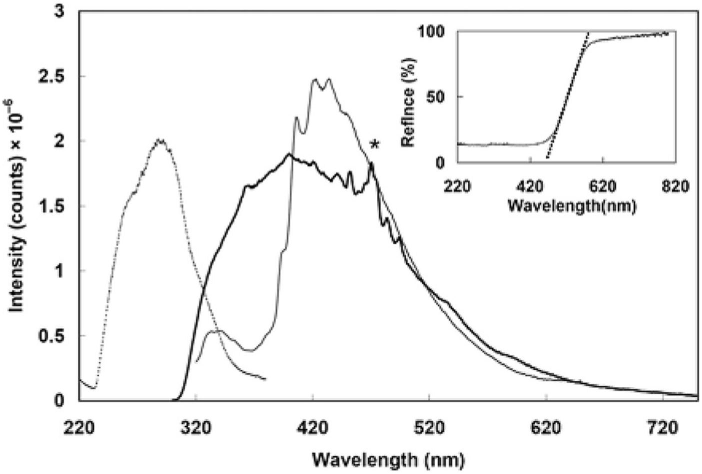

Figure 1. Photoluminescence spectra of complex **2**: 50 μM solution measured in MeTHF glass at 77 K, excitation ($\lambda_{em} = 435$ nm) (· · · ·); emission ($\lambda_{ex} = 285$ nm) (—); solid microcrystalline sample at 298 K, emission ($\lambda_{ex} = 250$ nm) (**—**). Inset shows diffuse-reflectance UV-vis spectrum for microcrystalline sample at 298 K, which gives band gap at 470 nm ($E_g = 2.66$ eV) denoted with a * on the solid state emission spectrum.

Our first foray into the arena of optoelectronically active metallacarboranes was marked by the observation that complex **2** was strongly emissive in 2-methyltetrahydrofuran (MeTHF) glass at 77 K as well as in the solid state at room temperature (Figure 1).[23] The UV excitation ($\lambda_{ex} = 285$ nm) leading to the observed emission of blue light at $\lambda_{em} = 435$ nm at 77 K appeared to correspond to a Re^{I}-NO^{+} MLCT transition, an absorption similarly ascribed in the cyclopentadienide analog $[Re(NO)(CO)_2(\eta^5\text{-}C_5H_5)][PF_6]$.[24] Some vibrational fine structure ($\Delta\nu \approx 800\ cm^{-1}$) in the emission profile was attributed to carborane B−H bending modes corresponding with the observation in DFT calculations of some ground state Re^{I} *d*-electron density delocalization onto the cage. Photoexcitation of solid microcrystalline samples at wavelengths below 300 nm produced a broad, intense emission at $\lambda_{em} \approx 400$ nm (Figure 1). Of note with this behavior was the consistent observation of a band edge spike at $\lambda = 470$ nm, which matched up with the band gap detected by diffuse-reflectance UV-vis measurement ($E_g = 2.66$ eV).

Earlier studies on this complex by Bitterwolf et al. had revealed some fascinating photochemical processes in Nujol or MeTHF matrices at

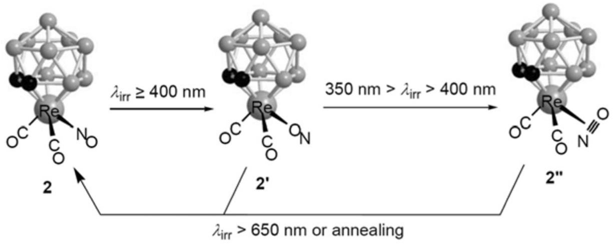

Scheme 1. Photochemically produced linkage isomers of complex **2**: **2** = nitrosyl; **2′** = isonitrosyl; **2″** = η^2-nitrosyl.

77 K, which could be stimulated by course tuning of the near-UV-vis irradiating wavelengths of light.[25] Thus at $\lambda_{irr} \geq 400$ nm isomeric conversion to the oxygen-bound terminal NO was observed, while further photolysis at $350\,nm < \lambda_{irr} < 400\,nm$ yielded a side-on bound η^2-NO, both processes being reversible (Scheme 1).

At about the same time, we described the synthesis of a halo-modified analog of compound **1**. Thus iodination of **1** with elemental I_2 followed by treatment with just about any kind of donor molecule (*e.g.* THF) afforded a rearrangement from metal-bound iodide to β-B-iodinated carborane ligand in the compound [Z][3,3,3-$(CO)_3$-8-I-*closo*-3,1,2-$ReC_2B_9H_{10}$] (**3a**, $Z^+ = NEt_4^+$; **3b**, $Z^+ = [Fe(\eta^5\text{-}C_5H_5)_2]^+$) (Scheme 2).[23,26]

The reaction that formed **3** appeared to have been driven by strong soft–soft bonding between the boron and iodine atoms as well as the incredible stability of the regenerated $Re(CO)_3$ vertex in the *closo*-3,1,2 ReC_2B_9 cluster. Despite this seemingly subtle transformation (the net change is a simple iodination of the β-B vertex), the impact on the optoelectronic properties of the complex was quite profound. While

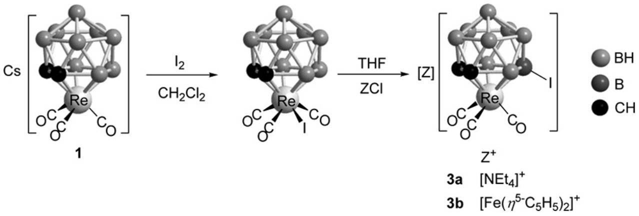

Scheme 2. Carborane cage iodination of the complex anion of **1** to afford compound **3**.

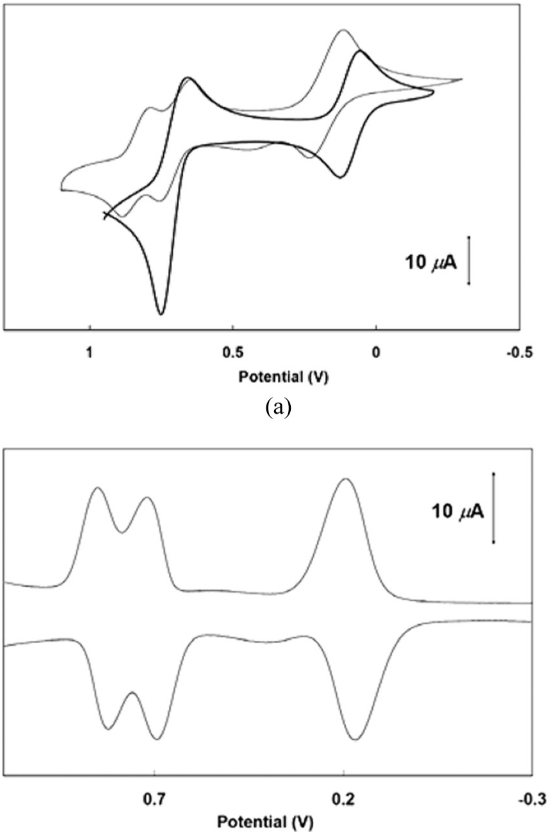

(b)

Figure 2. (a) CV of 652 μM solutions of compound **3b** in MeCN (**—**) and CH_2Cl_2 (—) at a scan rate of 0.1 V s^{-1}. (b) DPV of a 652 μM solution of compound **3b** in CH_2Cl_2. Both positive (bottom) and negative (top) scan polarities are shown. Note compound **3b** has incorporated ferrocenium ($[Fe(\eta^5\text{-}C_5H_5)_2]^+$) as the countercation.

compound **1** was non-emissive (in any solvent at any temperature) and was irreversibly oxidized in MeCN or CH_2Cl_2 solution (as measured by cyclic voltammetry (CV) and differential pulse voltammetry (DPV)), complex **3** displayed a quasi-reversible 2-electron oxidation in MeCN or two sequential, fully reversible oxidations in CH_2Cl_2 (Figure 2). Thus the former solvent promoted a 2-electron oxidation, which was likely followed by solvent ligation of the resulting Re^{III} complex. The solvent CH_2Cl_2, on the other hand, clearly favored separate 1-electron

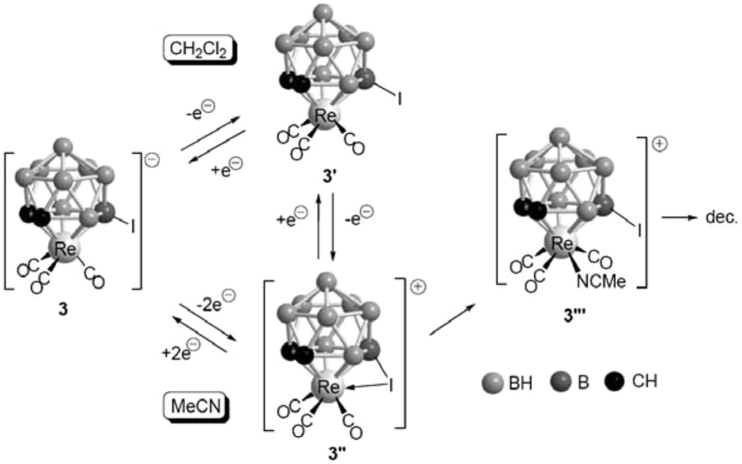

Scheme 3. $\vec{\mathbf{E}}\vec{\mathbf{E}}C_{\mathrm{rev}}$ and $\vec{\mathbf{E}}C_{\mathrm{rev}}C_{\mathrm{irrev}}$ mechanisms in the electrochemical oxidation of compound 3 in CH_2Cl_2 and MeCN.

oxidations through the intermediacy of a viable and observable neutral Re^{II} intermediate. In either case the presence of the β-B-bound iodine must have stabilized the oxidized products substantially versus the precursor complex in compound **1**, the most likely scenario being an intramolecular $B{-}I \rightarrow Re$ bridge between the β-B atom and the Re^{III} metal center, as electrochemical measurements enabled us to rule out any kind of dimerization (Scheme 3).

Although weakly emissive in solution at ambient temperature, in MeTHF glass at 77 K, bright phosphorescence was observed at $\lambda_{em} = 455$ nm resulting from excitation at $\lambda_{ex} = 275$ nm (Figure 3a). The latter appeared to manifest itself as a sharp absorption ($\lambda_{max} = 270$ nm) in the UV-vis spectrum of complex **3** in THF solution at room temperature, a feature which the parent complex **1** lacked (Figure 3b).

Xenon flash lamp time-resolved measurements revealed a single-exponential lifetime decay of $\tau = 1.65$ ms, supporting the notion of a triplet state as the emissive species. This might have been entirely expected given the presence of the iodine, which afforded an additional internal heavy atom effect leading to enhanced spin-orbit coupling. Without transient absorption measurements, it was difficult to pinpoint the precise nature of the photoemissive behavior, but the broadness of the emission peak was suggestive of a ^3dd state. However, the energy

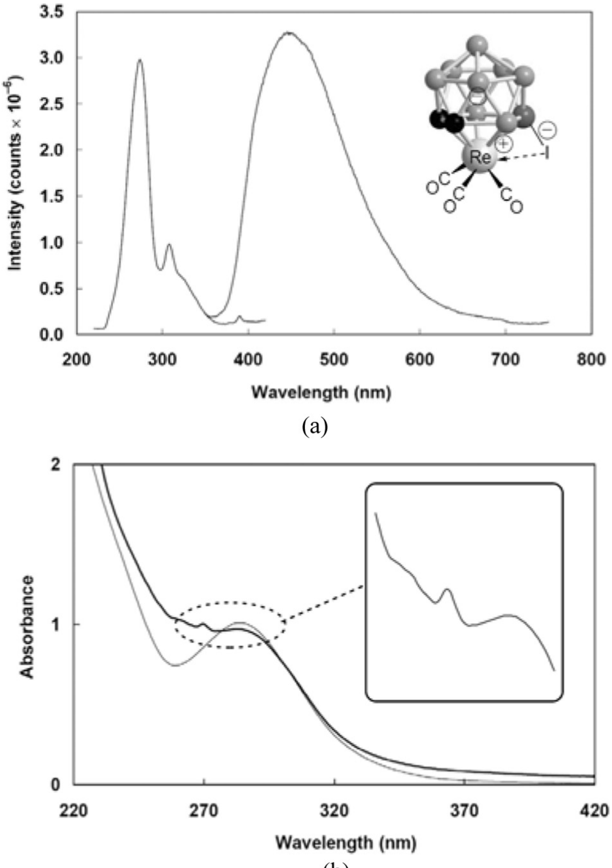

(a)

(b)

Figure 3. (a) Photoluminescence spectra of a 50 μM solution of compound 3 measured in MeTHF glass at 77 K: excitation ($\lambda_{em} = 455$ nm); emission ($\lambda_{ex} = 275$ nm). Inset shows a tentative structure for the postulated excited state exciplex. (b) UV-vis absorption spectra of 250 μM THF solutions of compound 3 (**—**) and compound 1 (—). Inset shows expansion of the curve for compound 3 between *ca.* 260 to 290 nm.

and strength of the absorption and the relatively high energy of the emission suggested significant ligand perturbation was likely. Thus mixing of the highest lying Re *d* orbitals with ground state carborane cage and carbonyl orbitals was likely to impact the energy of photoexcitation and emission. In order to account for the observed optical response at 77 K, we coupled our electrochemical observations with those of the photophysical analysis to suggest that a distorted Re → B−I σ^*

intramolecular exciplex was forming, with some degree of iodine-lone-pair-metal interaction to offset the charge transfer. This supported the fact that there was little dependence of the absorption at $\lambda_{\mathrm{max}} = 270$ nm on solvent polarity. On reflection, we realized that this mechanism may have been an over-simplification and that the nature of the orbital that became occupied in the excited state was not so certain and may not be purely B–I σ^* antibonding (and thus boron-centered owing to the electronegativity difference between boron and iodine), but a somewhat more complicated, diffuse MO on the carborane cage. Our subsequent work with ruthenacarboranes (vide infra) lended support to this notion.

2.2. Ruthenacarborane Work

In the year following our first reports of these luminescent rhenacarborane complexes, we decided to exploit the chemistry of another complex whose reactivity had been thoroughly investigated by the Stone laboratory. We discovered that the carbonyl ligands of the complex [3,3,3-$(CO)_3$-*closo*-3,1,2-$RuC_2B_9H_{11}$] (**4**) could be labilized and substituted by treatment with 2 molar equivalents of Me_3NO.[27] In the presence of 2,2′-bipyridyls, the complexes [3-CO-3,3-{κ^2-4,4′-R_2-2,2′-$(NC_5H_3)_2$}-*closo*-3,1,2-$RuC_2B_9H_{11}$] (**5a**, R = H; **5b**, R = $(CH_2)_8Me$; **5c**, R = Bu^t) were formed, while if TMEDA (*N*,*N*,*N*′,*N*′-tetramethylethylenediamine) were employed, the complex [3-CO-3,3-{κ^2-$Me_2N(CH_2)_2NMe_2$}-*closo*-3,1,2-$RuC_2B_9H_{11}$] (**6**) could be synthesized using the same methodology. Our initial and somewhat naïve hypothesis was that the 2,2′-bipyridyl complexes **5** would demonstrate the most interesting photophysical properties, given the rich optoelectronic chemistry of 2,2′-bipyridyl complexes of Ru^{II}, such as the archetypal [Ru{κ^2-2,2′-$(NC_5H_3)_2$}$_3$]$^{2+}$ complex ion.

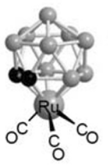

4

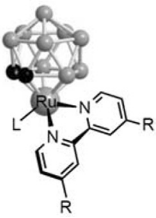

	L	R
5a	CO	H
5b	CO	$(CH_2)_8Me$
5c	CO	Bu^t
5a′	NCMe	H
5b′	NCMe	$(CH_2)_8Me$
5c′	NCMe	Bu^t

● BH ● CH

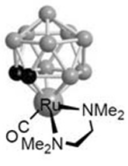

6

All the complexes **5** and **6** behaved electrochemically much as we would have suspected, at least in terms of outward appearance of their CVs. Thus in MeCN complexes **5** demonstrated two sequential

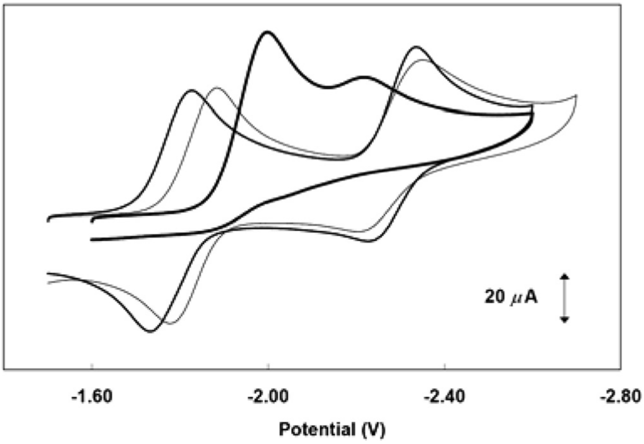

Figure 4. Reductive-cathodic CVs (scan rate 1.00 V s^{-1}) for MeCN (1.0 mM) solutions of complexes **5a** (——), **5c** (——), and **6** (——).

one-electron reductions with complex **6** not surprisingly undergoing an irreversible reduction (Figure 4).

Based on these observations, we initially and mistakenly assumed that the site of reduction in complexes **5** was the 2,2′-bipyridyl ligand, as is commonly found in 2,2′-bipyridyl complexes of Ru^{II}. However, spectroelectrochemical measurements of the reduction process and EPR analysis of the monoreduced product strongly suggested that the first (and likely the second) electron reduction sites were located on the metallacarborane cage framework, and not the 2,2′-bipyridyl ligand. For example, the reduced species **5c**$^-$ revealed a ν_{max}(CO) stretch at 1920 cm^{-1}, just 40 cm^{-1} less than the neutral parent (ν_{max}(CO) = 1960 cm^{-1}) (Figure 5a). More telling was the EPR spectrum of **5c**$^-$, which indicated a conspicuous absence of nitrogen hyperfine splitting, expected when an unpaired electron is confined to a single 2,2′-bipyridyl ligand (Figure 5b). The near-isotropic envelope observed for the solid sample of **5c**$^-$ was also consistent with a heavily delocalized metal *d*-carborane antibonding SUMO.

The oxidative behavior of the complexes **5** and **6** was also interesting and some important chemical reactivity was almost missed on our part. The latter complex **6** underwent an expected reversible $Ru^{III/II}$ oxidation in MeCN, but we were somewhat surprised to note that the complexes **5** were completely irreversibly oxidized at around the same potential in the same solvent (Figure 6).

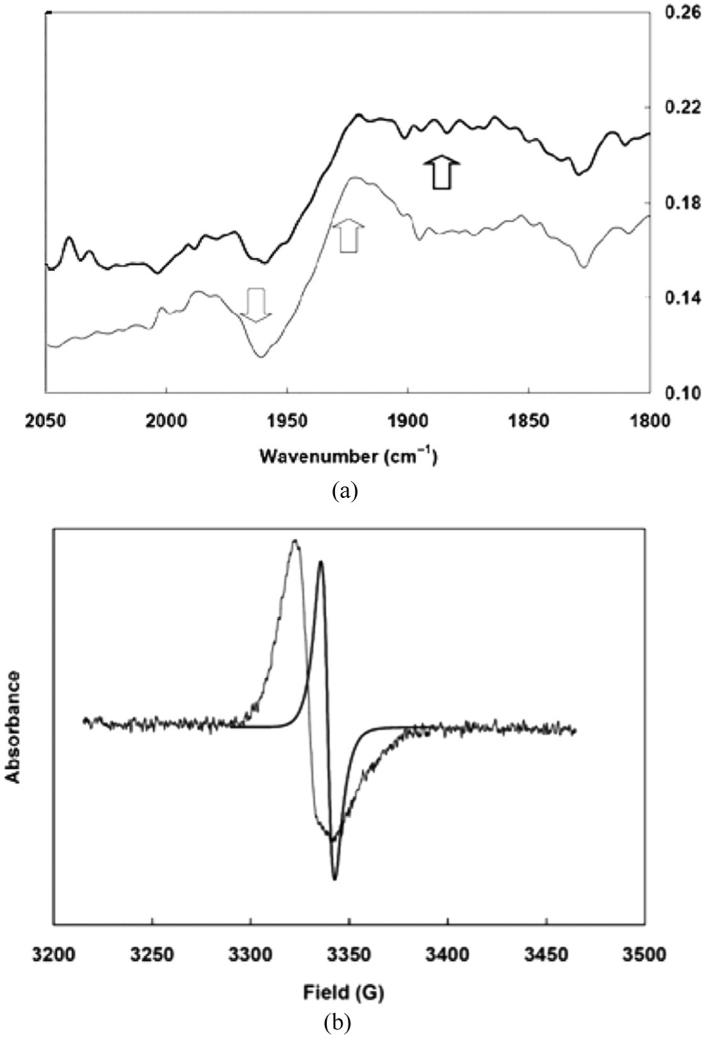

Figure 5. (a) Difference CA-IR spectra for the reduction of a solution of complex **5c** in MeCN (1.0 mM): potential held at –1.70 V (——); –2.30 V (▬▬). (b) X-band EPR spectra (298 K) of complex **5c** following reduction with 1 mol equiv. $NaC_{10}H_8$: THF (94 mM) solution (▬▬), $g_{iso} = 1.9972$; microcrystalline solid sample (——), $g_{1,2} = 1.9995$, $g_3 = 1.9925$.

Spectroelectrochemical analysis, again coupled with EPR analysis of the oxidized product **6**$^+$, strongly suggested a metal-centered oxidation, with substantial hyperfine splitting ($A_N = 0.45\,\mathrm{mT}$) of the unpaired

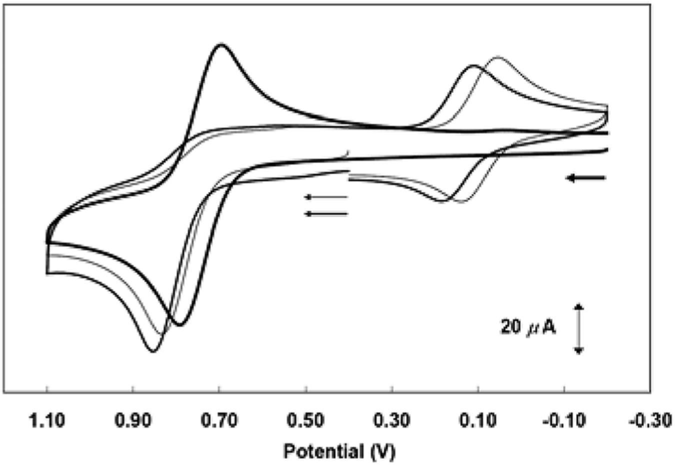

Figure 6. Oxidative-anodic CVs (scan rate 1.00 V s^{-1}) of MeCN (1.0 mM) solutions of complexes **5a** (——), **5c** (——), and **6** (▬▬).

electron by the metal-bound nitrogens of the TMEDA ligand (Figure 7). The change in ν_{max}(CO) of *ca.* + 100 cm^{-1} was particularly indicative of a metal-based oxidation.

For the 2,2′-bipyridyl complexes **5**, rather fortuitous widening of the CV scan range revealed a new reversible redox process some 0.7 V lower in potential, pursuant to the irreversible oxidation (a valuable lesson was learned here). This time spectroelectrochemical analysis indicated a considerably smaller positive shift in ν_{max}(CO) of only 37 cm^{-1} (Figure 8). Furthermore, the rate of growth of the CO absorption for **5**$^{+}$ was notably slower than that for the consumption of the neutral precursor **5**. Hence, it was very likely that the CO was being labilized in **5**$^{+}$ and dissociating to be replaced by the solvent. If CVs were run in MeCN, then this coordinating solvent was affording observable products **5′**$^{+}$, which then displayed (following some diffusion away from the electrode as confirmed by simulation) the almost-missed reversible $Ru^{III/II}$ couple at 0.7 V lower potential. Very importantly, we believed that the change in ν_{max}(CO) for complexes **5** and **6** upon one-electron oxidation could only be accounted for by a structural deformation that occurred for complexes **5** but not **6**, namely that of a *closo* → *isocloso* polyhedral rearrangement (Scheme 4). Stone *et al.* have previously observed this kind of

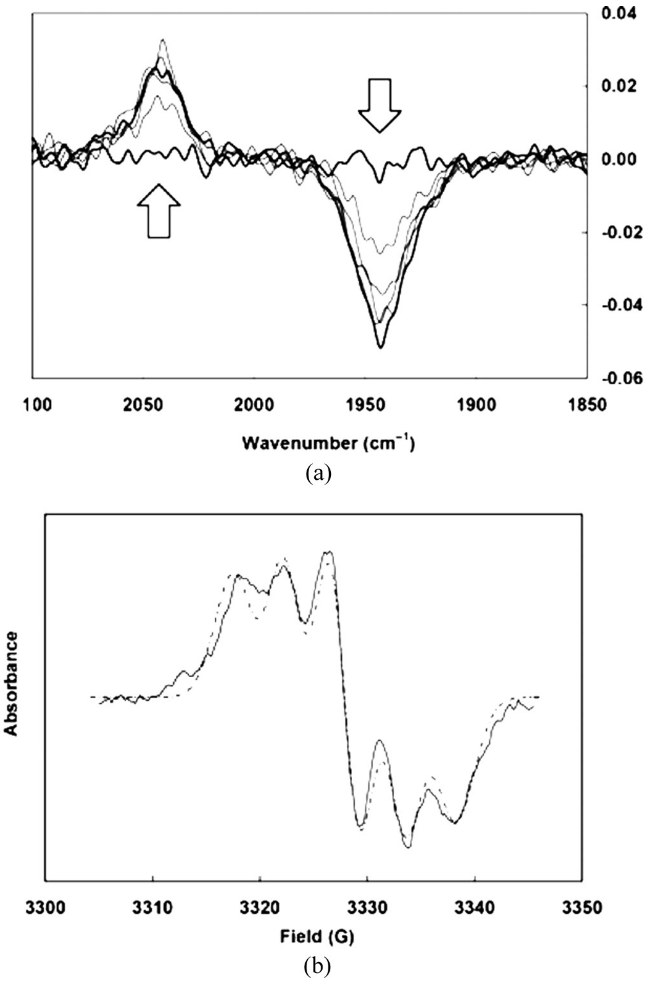

Figure 7. (a) Difference CV-IR spectra for the oxidation of a 1.0 mM solution of complex **6** in CH_2Cl_2 with the potential cycled between 0.8 and 1.3 V (0.8 V s^{-1}). (b) X-band EPR spectra (298 K) of complex **6** following oxidation with 0.9 mol equiv. $[N(C_6H_5Br\text{-}4)_3][SbCl_6]$. Sample in CH_2Cl_2 (26 mM) solution: (——) measured spectrum; (-·-·-·-) simulated spectrum, $g_{iso} = 2.0031$, $A_N = 0.45$ mT, linewidth = 0.40 mT.

structural reorganization for *closo*-3,1,2-MC_2B_9 systems, where a boron from the upper B_5 pentagonal belt migrates to within bonding distance of the metal, at the expense of the cage C–C connectivity.[28,29] We rationalized this process for complexes **5** and **6** in terms of simple

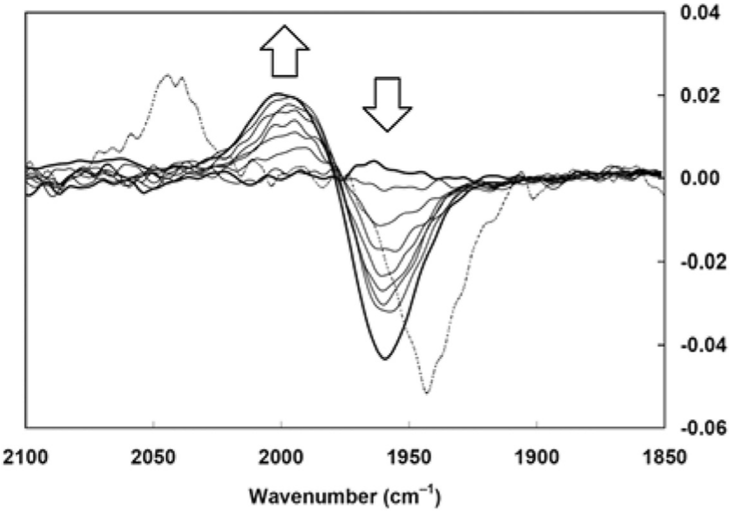

Figure 8. Difference CV-IR spectra for the oxidation of a 1.0 mM solution of complex **5c** in CH_2Cl_2. Sampled over the first minute of potential cycling (0.7–1.3 V, 0.80 V s^{-1}). For comparative purposes, the final measurement for the spectroelectrochemically observed oxidation of **6** is included (- - - - -).

Wade-Williams rules[30,31] arguments: an induced deficiency of polyhedral skeletal electrons (PSE) should stimulate the rearrangement depending on the donor ability of the κ^2-*N*-donor ligands. For 2,2′-bipyridyl, the poorer donor, the *closo* architecture cannot be preserved, the *closo* → *isocloso* modification occurs and CO loss ensues in the oxidized species. For TMEDA, a stronger if somewhat bulkier κ^2-donor,

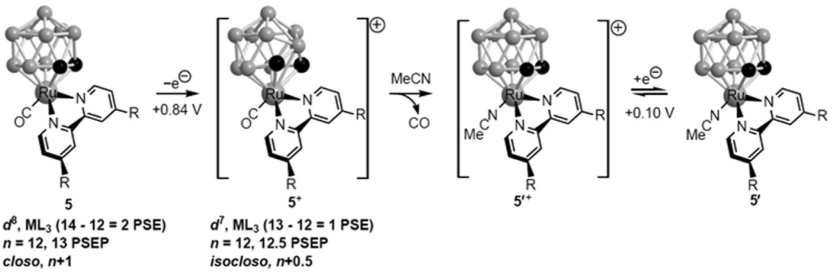

Scheme 4. Substitution lability upon electrochemical oxidation of the complexes **5** in MeCN.

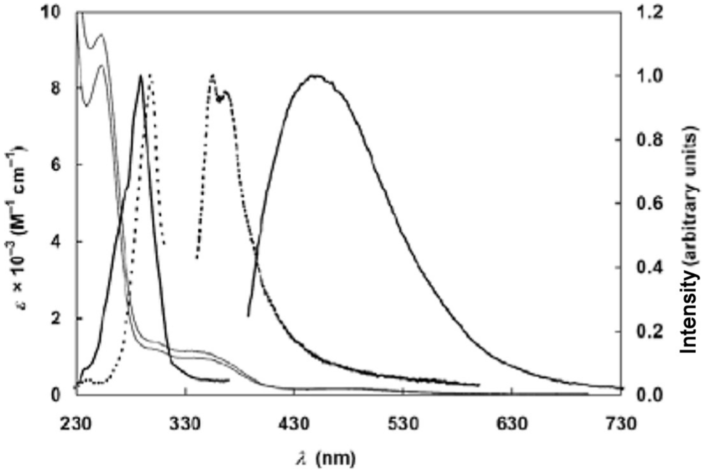

(a)

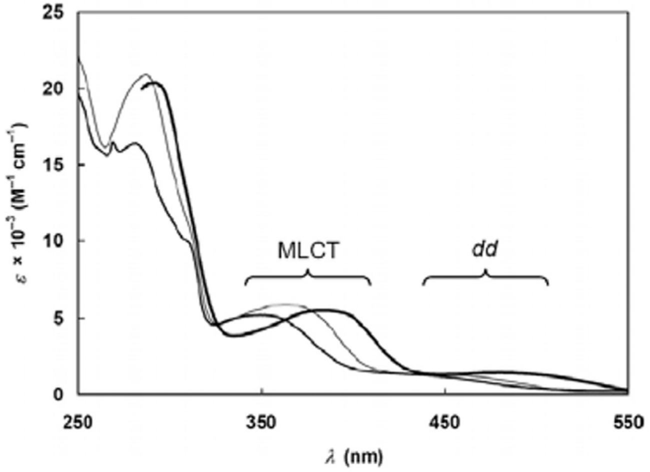

(b)

Figure 9. (a) UV-vis absorption spectra (——) for complex **6**, measured in MeCN and CH_2Cl_2 (left ordinate). Photoexcitation and emission spectra measured in THF (0.5 mM) at 298 K (- - - - -) and in MeTHF (50 μM) at 77 K (——) (right ordinate). Solvent-shifted Raman bands have been omitted. (b) UV-vis absorption spectra for complex **5c**, measured in MeCN (——), CH_2Cl_2 (—), and toluene (——).

the electron density at the metal in 6^+ is still elevated enough to maintain the *closo* structure and $d\pi^*$-backbonding is sufficient to curtail CO loss, at least on the CV timescale.

Spectroelectrochemical and EPR probing has in part helped us interpret some important facets of the molecular orbital structures of complexes **5** and **6** and subsequently to understand their observed photophysical responses. Far from displaying interesting photophysical properties, the 2,2′-bipyridyl complexes **5** are completely non-luminescent at any temperature. Complex **6**, on the other hand, while only weakly emissive at room temperature, was strongly phosphorescent in MeTHF glass at 77 K ($\lambda_{em} = 450$ nm, $\lambda_{ex} = 290$ nm, $\tau = 0.77$ ms) with features that were reminiscent of the photoemission from complex **3** (Figure 9a).

The optically benign nature of complexes **5** was straightforwardly attributed to the presence of *dd* states lower in energy than the MLCT transitions normally responsible for Ru-polypyridyl phosphorescence (Figure 9b). These *dd* states are of course significantly perturbed by backbonding with both the carborane and carbonyl ligands and are primarily responsible for efficient nonradiative dispersion of energy. MLCT states are necessarily absent for complex **6** and the observed emission is very characteristic of a *dd* triplet state. The question then arose as to why the *dd* states for complex **6** were photoemissive, while those of complexes **5** were not. Again we believed the answer may be rooted in simple Wade-Williams electron-counting rules. We knew that oxidation of complexes **5** resulted in an $n+1 \rightarrow n+0.5$ adjustment in PSE, sufficient to cause CO loss by virtue of a depletion of electron density at the metal. Photoexcitation of the complexes **5** promoted an electron from

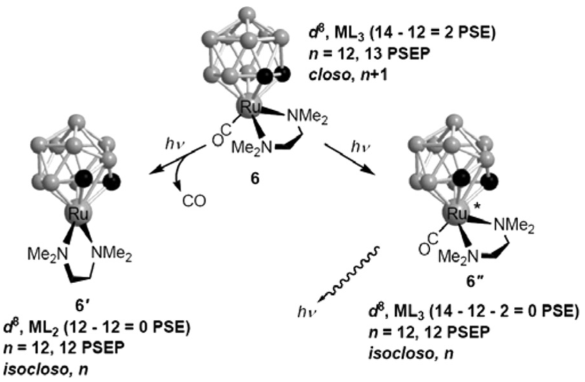

Scheme 5. Photochemical and -physical excitation of complex **6**.

a mostly metal *d* orbital to a carborane-delocalized antibonding MO (we knew this from the spectroelectrochemical and EPR measurements mentioned above), which represented a formal $n+1 \rightarrow n$ (*closo* → *isocloso*) change. One might therefore continue to expect photodissociation to dominate, even at 77 K. We also knew that complex **6** tolerated one-electron oxidation much better than the complexes **5**, we believed without any associated distortion of the metallacarborane cage framework. Thus the same $n+1 \rightarrow n$ photoexcitation of complex **6**, which was arguably more disruptive to the polyhedral skeletal bonding than the one-electron oxidation, may have resulted in a more photostable *isocloso* species leading to either photodissociation (**6′**) or the observed emissive triplet manifold (**6″**) (Scheme 5). In this respect, complex **6** does indeed share similar distorted d^6 metallacarborane photophysical characteristics with complex **3**, although we note here that complex **6** phosphoresces without the benefit of an additional heavy atom effect, namely that of iodine.

2.3. Recent Rhenacarborane Work

Up to now, our only observations of photoluminescence have been in frozen solvent glasses at 77 K. We still wondered whether or not one might observe ambient temperature solution luminescence from a metallacarborane, and quite by accident, we have succeeded in doing so.

The discovery that oxidation of complex **1** with elemental iodine could ultimately lead to iodination of the β-B vertex in a re-reduced Re^{I}-carborane $[3,3,3\text{-}(CO)_3\text{-}8\text{-}I\text{-}\textit{closo}\text{-}3,1,2\text{-}ReC_2B_9H_{10}]^-$ (**3**) was accompanied by work on another oxidation reaction employing the commercially-known reagent "Magic Blue," or more formally the ammoniumyl salt $[N(C_6H_5Br\text{-}4)_3][SbCl_6]$.[26] Due to the non-innocence of the $SbCl_6^-$

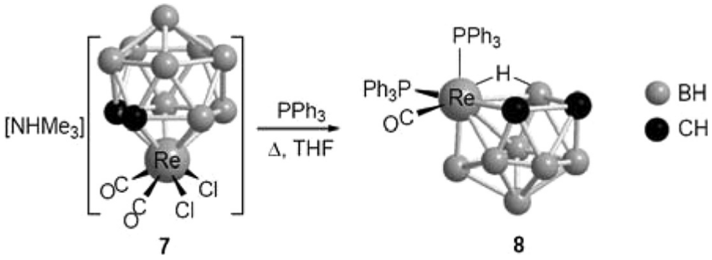

Scheme 6. Synthesis of complex **8**.

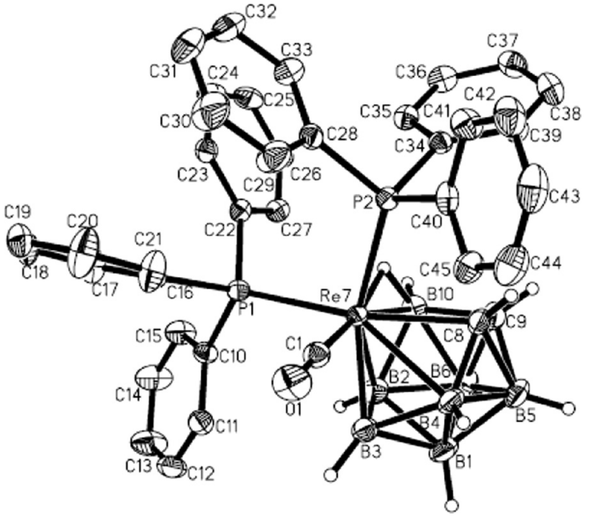

Figure 10. X-ray structure of complex **8**.

counterion (which we believe was oxidizing a transient neutral moiety, [3,3,3-$(CO)_3$-*closo*-3,1,2-$ReC_2B_9H_{11}$] (**1**–*e*), and with some additional help of the CO-abstracting reagent Me_3NO, we isolated the compound [$NHMe_3$][3,3-Cl_2-3,3-$(CO)_2$-*closo*-3,1,2-$ReC_2B_9H_{11}$] (**7**) in good yield. It was not certain what prompted us to investigate the reactivity of this compound with simple phosphines, but rather fortuitously, we found that simple refluxing of **7** with PPh_3 in THF afforded a remarkable new metallacarborane compound [7,10-μ-H-7-CO-7,7-$(PPh_3)_2$-*isonido*-7,8,9-$ReC_2B_7H_9$] (**8**) (Scheme 6).[32]

The most striking feature structurally was the degradation of the carborane cage by two boron vertices to give an *isonido*-7,8,9-ReC_2B_7 architecture. The open $\overline{\mathrm{ReCCB}}$ quadrilateral face was revealed by a single-crystal X-ray diffraction study (Figure 10) and the bridging Re–H–B endopolyhedral hydrogen atom in that face was spectroscopically observed in the ^1H NMR spectrum (*δ*–7.61).

Electrochemical measurements on CH_2Cl_2 solutions of complex **8** displayed what appeared to be a fully reversible one-electron oxidation, but distortions of the CV trace at high scan rates indicated that the process was not a simple electron transfer (Figure 11). Of course it was surprising to us that a formally Re^{III} metallacarborane complex could even

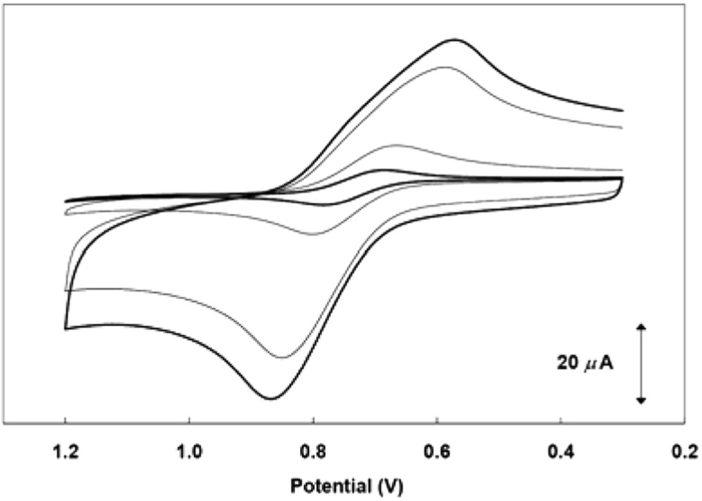

Figure 11. CVs for a CH_2Cl_2 solution (0.68 mM) of complex **8** at scan rates 0.02, 0.10, 1.00, and 1.50 V s^{-1} relative to Ag/$AgNO_3$ (MeCN, 10 mM).

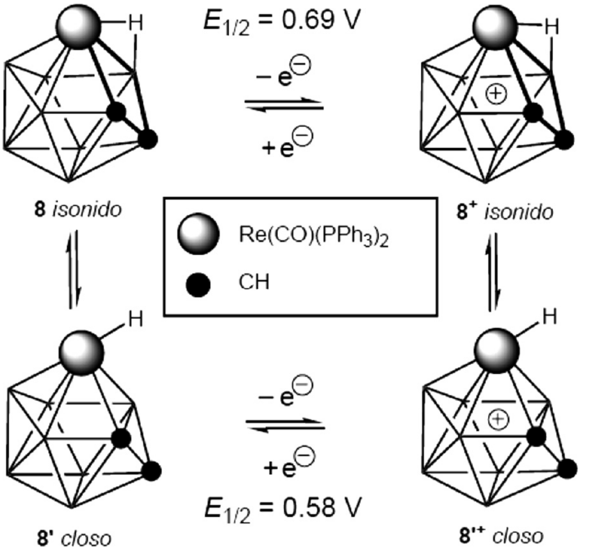

Scheme 7. Square scheme ($\vec{\mathbf{E}}C_{\text{rev}}\overleftarrow{\mathbf{E}}$) mechanism in the oxidation of complex **8**. Potentials quoted relative to ferrocene.

undergo such oxidation to a Re^{IV} cationic species without some indication of CO lability. Recall that the ruthenium complexes **5** with their comparatively more powerful donor 2,2′-bipyridyl ligands were distinctly labile in their oxidized Ru^{III} cationic state (*vide supra*). Simulation studies along with, once again, an educated interpretation of the Wade-Williams counting rules allowed us to devise a simple $\vec{\mathrm{E}}C_{\mathrm{rev}}\overleftarrow{\mathrm{E}}$ square scheme for the oxidation of complex **8** (Scheme 7). Our rationale was that complex **8** ought to comprise a *closo* (fully deltahedral) framework by those counting rules. The loss of an electron to give $\mathbf{8}^{+}$ was thus followed by a subtle polyhedral rearrangement to connect the *trans*-facial boron and carbon atoms. The new *closo* geometry $\mathbf{8}'^{+}$ displayed a slightly more cathodic response upon the return CV scan, the consequence of which was to reopen the cage back to the *isonido* geometry.

More surprisingly, complex **8** displayed ambient temperature luminescence in CH_2Cl_2 solution ($\lambda_{em} = 442$ nm) with an impressive quantum yield ($\Phi = 0.012$, following self-absorbance correction) for an organometallic complex (Figure 12). Solutions of complex **8** in this

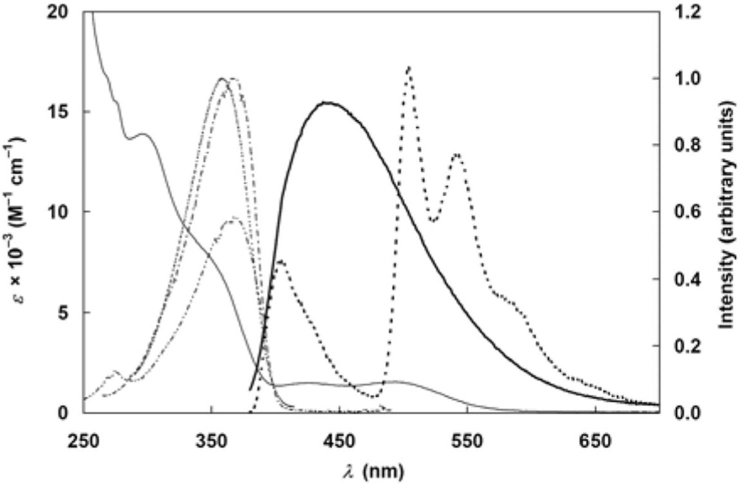

Figure 12. UV-vis spectrum of complex **8** in CH_2Cl_2 (50 μM) (—) (left ordinate). Photoluminescence spectra in CH_2Cl_2 (50 μM, 298 K): excitation ($\lambda_{em} = 442$ nm) (· · · ·); emission ($\lambda_{ex} = 360$ nm) (**—**). Photoluminescence spectra in MeTHF (50 μM, 77 K): excitation ($\lambda_{em} = 405$ nm) (— ● ● —); excitation ($\lambda_{em} = 504$ nm) (— ● —); emission ($\lambda_{ex} = 368$ nm) (- - -). Photoluminescence intensity (right ordinate) normalized relative to maximum excitation intensities.

and other solvents all demonstrated bright turquoise-blue luminescence when placed over a hand-held long-wavelength UV lamp.

Although the photoemission profile was broad, the UV-vis absorption and photoexcitation spectra ($\lambda_{ex} = 360$ nm) suggested that this was not due to *dd* phosphorescence. This was corroborated by pulsed laser time-resolved measurements, which revealed a variable, biexponential fluorescent decay with essentially a sub-nanosecond time regime—*e.g.* at the emission peak (442 nm), $\tau_1 = 0.44$ ns (74%) and $\tau_2 = 1.1$ ns (26%). Measurements in MeTHF glass at 77 K exposed dual fluorescent singlet manifolds, with a higher energy violet emission at $\lambda_{em} = 405$ nm ($\tau_1 = 0.18$ ns (92%) and $\tau_2 = 0.74$ ns (8%)) and an even more intense lower energy green emission at $\lambda_{em} = 504$ nm ($\tau_1 = 0.40$ ns (88%) and $\tau_2 = 4.7$ ns (12%)). Both emissions displayed vibronic structure, with the lower energy emission clearly resolved enough to quantify this at $\Delta\nu \approx 1400\ \mathrm{cm}^{-1}$. This fortunately provided a strong clue as to the nature of these excited singlet states, with absorptions in the ground state IR spectrum of **8** at 1430 and 1434 cm^{-1} assigned to aryl C$-$C *n* stretching modes in the phosphines. After ruling out a number of options for identifying the chromophore, a $\sigma_{\mathrm{ReP}} \rightarrow \sigma_{\mathrm{PC}^*}$ transition was assigned as the primary photoexcitation leading to the first (higher energy) singlet manifold $^1S_2$ (Scheme 8). Thus an electron was being excited from a metal-perturbed phosphine donor pair to one or more P–C σ^* orbitals, which we believe accounted for the observed vibronic structure. This implied that the metal-bound phosphine was the active chromophoric center

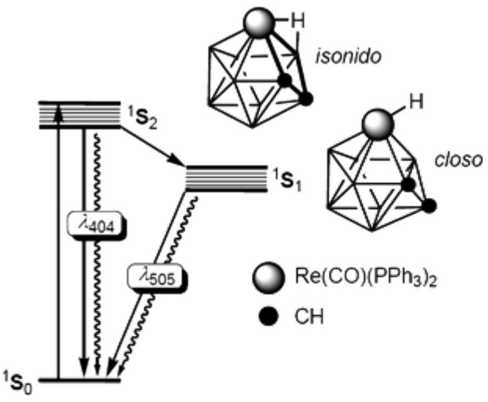

Scheme 8. Energy level diagrams for dual fluorescence of complex **8** at 77 K.

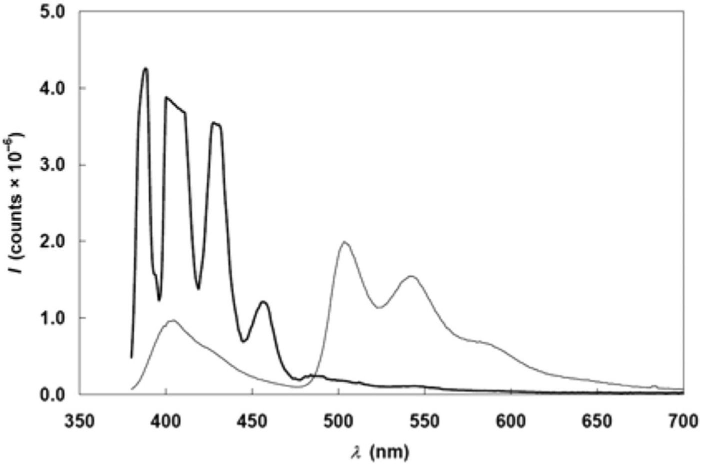

Figure 13. Photoluminescence spectra of complex **8** in MeTHF (50 μM, 77 K): emission ($\lambda_{ex} = 368$ nm) (—); in the presence of anthracene (10 mM) (▬▬).

rather that the carborane itself, which was nevertheless rather unique behavior for a Re^{III}-PR_3 complex. But to account for the dual fluorescence, there must have also been a subtle distortion of the complex to afford the second emissive singlet manifold, $^1S_1$. We can draw on our accompanying electrochemical measurements and our experiences with complexes **3** and **6** described above to suggest that this distortion again emanates from an $n+1$ *isonido* → *n closo* (or *isocloso*) transformation. This was logical from the perspective of a photoexcitation that displaces

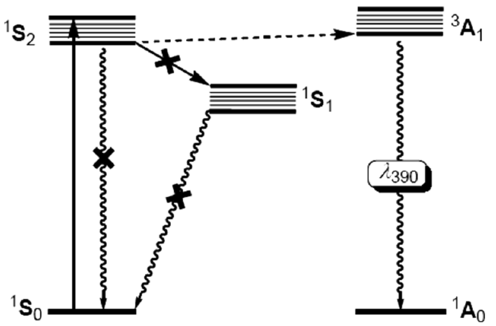

Scheme 9. Energy level diagrams for fluorescence quenching by singlet-triplet energy transfer to anthracene.

an electron from an orbital associated with polyhedral skeletal bonding, which the P → Re donor bond would be, to one that is completely exopolyhedral.

The $^1S_2$ state is well energy-matched with that of the anthracene triplet state $^3A_1$, and even at 77 K, with an excess of anthracene present in the solvent glass, we observed quenching of the $^1S_1$ emission (Figure 13), implying there must have been rapid and efficient intermolecular $^1S_2 \rightarrow {}^3A_1$ energy transfer ($k_{ET} > 10^9\,s^{-1}$) (Scheme 9). That was very interesting given the lack of translational molecular mobility and subsequent collisions one would expect at liquid nitrogen temperatures.

CONCLUSION

Without direct observation from measurements such as transient absorption spectroscopy, the excited state species responsible for the luminescent emissions described for complexes **3**, **6**, and **8** remain conjecture at the current time, but the circumstantial evidence for carborane cage plasticity influencing if not directly controlling optoelectronic properties appears to be mounting. What is clear from our work is that strongly luminescent metallacarborane complexes may now be synthesized. The scope for developing further optoelectronically active complexes is huge, bearing in mind that we have only employed two *d*-block metals in our studies so far—rhenium and ruthenium.

ACKNOWLEDGEMENTS

None of the work described here would have been possible without the dedicated contributions form my graduate students, Justin H. Orlando and Matthew J. Fischer, along with the much appreciated effort of undergraduate research assistants listed in the cited articles. Collaborations with researchers at other institutions have been vital in developing comprehensive, integrated descriptions of the complexes described. These include: Nigam P. Rath (X-ray crystallography, University of Missouri–St Louis); Michael J. Shaw (spectroelectrochemistry, Southern Illinois University at Edwardsville); Aleksander Siemiarczuk (time-resolved fluorescence measurements, Photon Technology Inc., Ontario, Canada). I am also indebted to my faculty colleagues at Saint Louis University, Steven W. Buckner and Shelley D. Minteer, for helpful discussions and advice. I am grateful to the following for financial support: Saint Louis

University; US government; Lynntech, Inc. Above all I am thankful to my former mentor, F. Gordon A. Stone, for providing me with the inspiration to work with these fascinating complexes.

REFERENCES

1. Hawthorne, M. F., D. C. Young, T. D. Andrews, D. V. Howe, R. L. Pilling, A. D. Pitts, M. Reintjes, L. F. Warren, Jr. and P. A. Wegner, 1968. *J. Am. Chem. Soc.*, **90**, 879.
2. Hawthorne, M. F., 1973. *Pure Appl. Chem.*, **39**, 475.
3. Callahan K. P. and M. F. Hawthorne, 1976. *Adv. Organomet. Chem.*, **14**, 145.
4. Grimes, R. N., 2000. *Coord. Chem. Rev.*, **200–202**, 773.
5. Hosmane, N. S., 2003. *Pure Appl. Chem.*, **75**, 1219.
6. Grimes, R. 1995. In *Comprehensive Organometallic Chemistry II*, Abel, E. W., F. G. A. Stone, G. Wilkinson, and C. E. Housecroft (eds.), vol. 1, pp. 373–430, Pergamon Press, Oxford, UK, Ch. 9.
7. Hosmane, N. S. and J. A. Maguire, 2006. In *Comprehensive Organometallic Chemistry III*, Crabtree, R. H., D. M. P. Mingos, and C. E. Housecroft, (eds.), vol. 3, pp. 175–264, Elsevier, Oxford, UK, Ch. 3.05.
8. Base, K. and M. W. Grinstaff, 1998. *Inorg. Chem.*, **37**, 1432.
9. Calhorda, M. J., O. Crespo, M. C. Gimeno, P. G. Jones, A. Laguna, J. M. López-de-Luzuriaga, J. L. Pérez, M. A. Ramón, and L. F. Veiros, 2000. *Inorg. Chem.*, **39**, 4280.
10. Hong, E., H. Jang, Y. Kim, S. C. Jeoung, and Y. Do, 2001. *Advanced Mater.*, **13**, 1094.
11. Weinstein, J. A., M. T. Tierney, E. S. Davies, K. Base, A. A. Robeiro, and M. W. Grinstaff, 2006. *Inorg. Chem.*, **45**, 4544.
12. Zhang, D., J. Dou, D. Li, and D. Wang, 2007. *J. Coord. Chem.*, **60**, 825.
13. Dou, J., D. Zhang, Y. Zhu, D. Li, and D. Wang, 2007. *Inorg. Chim. Acta*, **360**, 3387.
14. Kunkely, H. and A. Vogler, 2004. *Inorg. Chim. Acta*, **357**, 4607.
15. Kunkely, H. and A. Vogler, 2005. *Inorg. Chem. Commun.*, **8**, 992.
16. Crespo, O., C. Gimeno, P. G. Jones, A. Laguna, J. M. López-de-Luzuriaga, M. Monge, J. L. Pérez, and M. A. Ramón, 2003. *Inorg. Chem.*, **42**, 2061.
17. Zhang, D., J. Dou, D. Li., and D. Wang, 2006. *Inorg. Chim. Acta*, **359**, 4243.
18. Hawthorne, M. F., J. I. Zink, J. M. Skelton, M. J. Bayer, C. Liu, E. Livshits, R. Baer, and D. Neuhauser, 2004. *Science*, **303**, 1849.
19. Ellis, D. D., P. A. Jelliss, and F. G. A. Stone, 1999. *Organometallics*, **18**, 4982.
20. Ellis, D. D., P. A. Jelliss, and F. G. A. Stone, 2000. *J. Chem. Soc., Dalton Trans.*, 2113.
21. Ellis, D. D., J. C. Jeffery, P. A. Jelliss, J. A. Kautz, and F. G. A. Stone, 2001. *Inorg. Chem.*, **40**, 2041.

22. Ellis, D. D., P. A. Jelliss, and F. G. A. Stone, 1999. *J. Chem. Soc., Chem. Commun.*, 2385.
23. Fischer, M. J., P. A. Jelliss, J. H. Orlando, L. M. Phifer, and N. P. Rath, 2005. *J. Lumin.*, **114**, 60.
24. Kunkely, H., V. Pawlowski, and A. Vogler, 2002. *Inorg. Chim. Acta*, **335**, 147.
25. Bitterwolf, T. E., W. B. Scallorn, C. A. Weiss, and P. A. Jelliss, 2002. *Organometallics*, **21**, 1856.
26. Fischer, M. J., P. A. Jelliss, L. M. Phifer, and N. P. Rath, 2005. *Inorg. Chim. Acta*, **358**, 1531.
27. Jelliss, P. A., J. Mason, J. M. Nazzoli, J. H. Orlando, A. Vinson, N. P. Rath, and M. J. Shaw, 2006. *Inorg. Chem.*, **45**, 370.
28. Attfield, M. J., J. A. K. Howard, A. N. de M. Jelfs, C. M. Nunn, and F. G. A. Stone, 1987. *J. Chem. Soc., Dalton Trans.*, 2219.
29. Carr, N., D. F. Mullica, E. L. Sappenfield, and F. G. A. Stone, 1992. *Organometallics*, **11**, 3697.
30. Wade, K., 1976. *Adv. Inorg. Chem. Radiochem.*, **18**, 1.
31. Williams, R. E., 1976. *Adv. Inorg. Chem. Radiochem.*, **18**, 67.
32. Buckner, S. W., M. J. Fischer, P. A. Jelliss, R. Luo, S. D. Minteer, N. P. Rath, and A. Siemiarczuk, 2006. *Inorg. Chem.*, **45**, 7339.

Paul A. Jelliss is an associate professor in the Department of Chemistry at Saint Louis University. His research interests include synthesis, characterization and unusual structures and properties of organometallic complexes, especially metallacarboranes. He has published articles in *Inorganic Chemistry*, *Organometallics*, *Inorganica Chimica Acta*, and the *Journal of Materials Chemistry* as well as chapters in *Specialist Periodical Reports and Comprehensive Organometallic Chemistry III.*